

# REPORT DOCUMENTATION PAGE

Form Approved  
OMB No. 0704-0188

Public reporting burden for this collection of information is estimated to average 1 hour per response, including the time for reviewing instructions, searching existing data sources, gathering and maintaining the data needed, and completing and reviewing the collection of information. Send comments regarding this burden estimate or any other aspect of this collection of information, including suggestions for reducing this burden, to Washington Headquarters Services, Directorate for Information Operations and Reports, 1215 Jefferson Davis Highway, Suite 1204, Arlington, VA 22202-4302, and to the Office of Management and Budget, Paperwork Reduction Project (0704-0188), Washington, DC 20503.

1. AGENCY USE ONLY (Leave blank)	2. REPORT DATE	3. REPORT TYPE AND DATES COVERED	
	April 4, 1995	Final 1 Jun 92 - 31 Dec 94	
4. TITLE AND SUBTITLE		5. FUNDING NUMBERS	
Thermal Decomposition Pathways in Nitramine Propellants		ARO M1PR 126-94	
6. AUTHOR(S)		DTIC	
F. J. Lovas and R. D. Suenram		PERFORMING ORGANIZATION REPORT NUMBER JUL1101995	
7. PERFORMING ORGANIZATION NAME(S) AND ADDRESS(ES)		B	
National Institute of Standards and Technology Physics Laboratory - Molecular Physics Division, 843 B268 Physics Bldg. (221) Gaithersburg, MD 20899			
9. SPONSORING/MONITORING AGENCY NAME(S) AND ADDRESS(ES)		10. SPONSORING/MONITORING AGENCY REPORT NUMBER	
U.S. Army Research Office P.O. Box 12211 Research Triangle Park, NC 27709-2211		ARO 29596.2-CH	
11. SUPPLEMENTARY NOTES The views, opinions and/or findings contained in this report are those of the author(s) and should not be construed as an official Department of the Army position, policy, or decision, unless so designated by other documentation.			
12a. DISTRIBUTION/AVAILABILITY STATEMENT  Approved for public release; distribution unlimited.		12b. DISTRIBUTION CODE	
13. ABSTRACT (Maximum 200 words)  We have investigated intermediates and products in the thermal decomposition of RDX vapor, using a variety of experimental microwave techniques previously employed in our laboratory in studies of pyrolysis decomposition of organic amines. We used microwave spectroscopy to determine the chemical composition of the decomposition of nitramines by pyrolysis methods and identify the products in the thermal decomposition processes. The objective was to determine the validity of proposed decomposition mechanisms, and to identify new reaction products or pathways.			
DTIC QUALITY INSPECTED 5			
14. SUBJECT TERMS explosives; microwave; millimeterwave; pyrolysis, spectra		15. NUMBER OF PAGES 44	
		16. PRICE CODE	
17. SECURITY CLASSIFICATION OF REPORT UNCLASSIFIED	18. SECURITY CLASSIFICATION OF THIS PAGE UNCLASSIFIED	19. SECURITY CLASSIFICATION OF ABSTRACT UNCLASSIFIED	20. LIMITATION OF ABSTRACT UL

**THERMAL DECOMPOSITION PATHWAYS IN NITRAMINE PROPELLANTS**

**FINAL REPORT**

**F. J. Lovas and R. D. Suenram**

**March 31, 1995**

**U. S. Army Research Office**

**Contract Number 29596-CH**

**Physics Laboratory**

**Molecular Physics Division**

**National Institute of Standards and Technology**

**Gaithersburg, MD 20899**

**APPROVED FOR PUBLIC RELEASE;  
DISTRIBUTION UNLIMITED**

THE VIEWS, OPINIONS, AND/OR FINDINGS CONTAINED IN THIS REPORT ARE THOSE OF THE AUTHORS AND SHOULD NOT BE CONSTRUED AS AN OFFICIAL DEPARTMENT OF THE ARMY POSITION, POLICY, OR DECISION, UNLESS SO DESIGNATED BY OTHER DOCUMENTS.

Accession For	
NTIS	GRA&I <input checked="" type="checkbox"/>
DTIC TAB	<input type="checkbox"/>
Unannounced	<input type="checkbox"/>
Justification	
By _____	
Distribution/	
Availability-Codes	
Distr	Avail and/or Special

# THERMAL DECOMPOSITION PATHWAYS IN NITRAMINE PROPELLANTS

## TABLE OF CONTENTS

### Abstract

### I. Background

1. Nitramine Combustion and Decomposition Chemistry
2. RDX Decomposition - Photolysis Versus Thermal Decomposition

### II. Experimental Results

1. Pulsed-beam Fourier-Transform Experiments
  - A. Survey of RDX
  - B. Structure of Nitromethane-Water
2. Pyrolysis Studies of RDX - Microwave Studies
  - A. Temperature profiles
  - B. Species X - Assignment of Unidentified Species

### III. Conclusions

## LIST OF APPENDIXES, ILLUSTRATIONS AND TABLES

Figure 1. Pulsed-Nozzle Fourier-Transform Microwave (FTMW) Spectrometer

Figure 2a. Millimeterwave synthesizer frequency source

Figure 2b. Millimeterwave spectrometer with RDX pyrolysis source

Figure 3. Structure of nitromethane-water

Figure 4. Calculated spectrum of  $\text{CH}_2=\text{NNO}_2$

Figure 5. Observed spectra from RDX vapor decomposition

Figure 6. Spectral line intensity as a function of pyrolysis zone temperature

TABLE I. Microwave Transitions Identified in Heated Nozzle FTMW Study of RDX

TABLE II. Microwave Transitions Identified in Pyrolysis MW Study of RDX

TABLE III. Species Identified by Mass Spectrometry and Microwave Spectroscopy

TABLE IV. Species X Rotational Parameters

APPENDIX 1. Spectral Line Survey of RDX Decomposition Products

## Abstract

We have investigated intermediates and products in the thermal decomposition of RDX vapor, using a variety of experimental microwave techniques previously employed in our laboratory in studies of pyrolysis decomposition of organic amines. We used microwave spectroscopy to determine the chemical composition of the decomposition of nitramines by pyrolysis methods and identify the products in the thermal decomposition processes. The objective was to determine the validity of proposed decomposition mechanisms, and to identify new reaction products or pathways.

## I. Background

Nitramine propellants<sup>1</sup> are energetic chemical compounds containing nitro groups chemically bound to other nitrogen atoms, i.e., containing fragments of the form N-NO<sub>2</sub>. RDX (hexahydro-1,3,5-trinitro-1,3,5-triazine) and HMX (octahydro-1,3,5,7-tetranitro-1,3,5,7-tetrazine) are two of the most widely used propellants of this type, and considerable research exists on the macroscopic ignition and combustion properties of RDX and HMX<sup>2-7</sup>. In order to optimize the application of explosives such as RDX and HMX, as well as to devise improved propellants with related chemical properties, a knowledge of the microscopic ignition and combustion behavior of these propellants is required. Obtaining molecular level information on nitramine ignition and combustion in the high-pressure, high-temperature environments typical of actual propellant applications is not easy. It therefore makes sense to pursue an alternative strategy of obtaining information under more controlled laboratory conditions, and transferring this information to the harsher application

environments. We have employed microwave spectroscopy to determine with certainty the chemical composition of many of the products of thermal decomposition of RDX. Thermal decomposition was induced both by simple heating of the sample in a metal nozzle and by a rather gentle thermal pyrolysis technique in which the vapor of RDX is flowed over a heated catalytic substrate.

### 1. Nitramine Combustion and Decomposition Chemistry

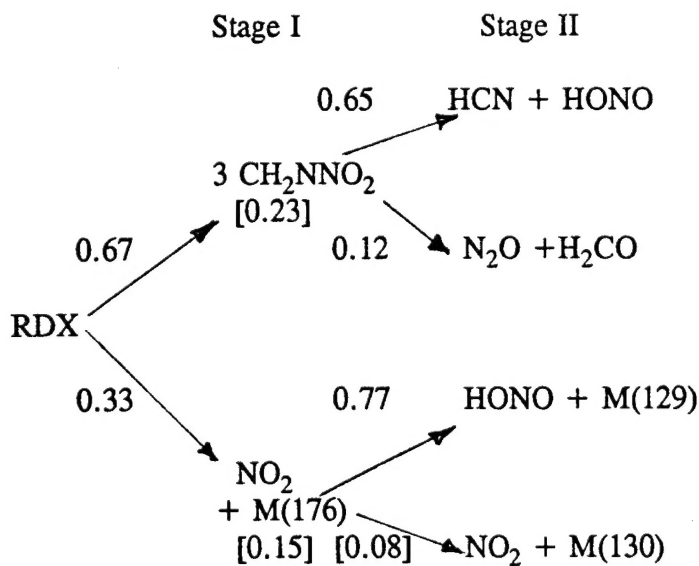
Detailed chemical kinetics mechanisms for ignition and combustion are not well known for any of the energetic propellants. Nevertheless, recent detailed chemical kinetics modelling efforts<sup>8-10</sup> have led to a global understanding for common nitramine propellants which is relatively successful. Melius<sup>8,9</sup> used a model containing 31 chemical species and 137 chemical reactions to reproduce species profiles, flame speed, and pressure dependence for a 0.05 MPa RDX flame. The success of this model suggests that efforts to make it more complete are desirable, and it is in this context that the present study of the chemical composition of early decomposition products should be viewed.

Zhao, Hintsza and Lee<sup>11</sup> used a time-of-flight (TOF) mass spectrometer to detect decomposition products after infrared multiphoton dissociation of RDX in a molecular beam in order to investigate the mechanism of RDX thermal decomposition. They determined photodissociation channels, branching ratios and translational energy distributions. In contrast to the conventional view before their work, i.e., the view that simple bond rupture through loss of NO<sub>2</sub> was the dominant primary channel in RDX thermal decomposition, Zhao, Hintsza and Lee found that the dominant primary channel of photodecomposition is a

concerted symmetric triple fission to produce three  $\text{CH}_2\text{N}_2\text{O}_2$  (mass 74) fragments, which subsequently undergo secondary concerted dissociation to produce HCN,  $\text{H}_2\text{CO}$ , HONO (or possibly the isomeric  $\text{HNO}_2$ ) and  $\text{N}_2\text{O}$ . A total of two primary and four secondary dissociation channels were observed.

## 2. RDX Decomposition - Photolysis Versus Thermal Decomposition

The reaction scheme described above has some parallels in the unimolecular laser infrared multiphoton dissociation (IRMPD) photolysis decomposition scheme for RDX proposed by Zhao, et al.<sup>11</sup> through deconvolution of the time-of flight mass spectra which is illustrated below:



The dominant channel is a concerted triple fission of the RDX ring to produce three  $\text{CH}_2\text{N}_2\text{O}_2$  (mass 74) fragments which was identified to be the  $\text{CH}_3=\text{NNO}_2$  species. Zhao et al.<sup>11</sup> contend that the dissociation mechanism obtained in IRMPD experiments is the same as that in thermal decomposition experiments on other moderate size systems they have investigated.

Recent pyrolysis studies by Behrens<sup>12-13</sup> on RDX and HDX, which employed thermogravimetric modulated beam and time-of flight mass spectrometry, suggest that decomposition in the liquid phase differs from the gas phase IRMPD experiments. Behrens found that both nitramines form H<sub>2</sub>O, N<sub>2</sub>O, CH<sub>2</sub>O, NO and (CH<sub>3</sub>)NHCHO. In addition, RDX produces NO<sub>2</sub> and hydroxy-s-triazine from N-N bond breaking while HMX forms C<sub>2</sub>H<sub>6</sub>N<sub>2</sub>O (mass 74), CO and a residue. Behrens argues that the mass 74, with stoichiometry of C<sub>2</sub>H<sub>6</sub>N<sub>2</sub>O, is not methylenenitramine (CH<sub>2</sub>N<sub>2</sub>O<sub>2</sub>) as suggested in the IRMPD study based on deuterium and <sup>15</sup>N labelling experiments, but they do not offer a molecular formula to explain this mass peak. All conceivable structures for this species would require bimolecular reactions since the N=O bond must be ruptured or modified by atom addition. The primary species produced in the thermal decomposition studies of liquid RDX are N<sub>2</sub>O, CH<sub>2</sub>O, and H<sub>2</sub>O, while secondary products are CO, NO, and HCN with minor products C<sub>2</sub>H<sub>5</sub>NO and C<sub>2</sub>H<sub>6</sub>N<sub>2</sub>O. Behrens and Bulusu<sup>14,15</sup> propose the following decomposition paths for liquid RDX at temperatures between 195° C and 215° C:

	<u>Path</u>	<u>Fraction</u>
RDX	OST <sup>a</sup> + H <sub>2</sub> O + NO + NO <sub>2</sub>	1 30%
[+NO]	NO <sub>2</sub> + H <sub>2</sub> CN + 2N <sub>2</sub> O + 2CH <sub>2</sub> O	2 10%
catalyst	ONDNTA <sup>b</sup> --> N <sub>2</sub> O + CH <sub>2</sub> O + other	3 35%
	N <sub>2</sub> O + CH <sub>2</sub> O + NO <sub>2</sub> + NH <sub>2</sub> CHO	4 25%

The first and second pathways are first-order reactions in the decomposition of RDX. Based on their time-of-flight spectra, they concluded that the products HCN, N<sub>2</sub>O, HONO, NH<sub>2</sub>CHO, and C<sub>3</sub>H<sub>3</sub>N<sub>3</sub>O (oxy-s-triazine) arise only from other decomposition products. The products CO, CH<sub>2</sub>O, NO and NO<sub>2</sub> show contributions from RDX and from other decomposition products. No direct evidence for formation of CH<sub>2</sub>=NNO<sub>2</sub> was reported, and the H<sub>2</sub>CN species in pathway 2 appears to have been added to account for the chemical

balance based on the RDX formula,  $C_3H_6N_6O_6$ . Thus, the RDX decomposition experiments studied by the thermogravimetric-mass spectroscopy methods yield dramatically different results than the IRMPD studies and leave many questions unanswered. Mass spectroscopic investigations such as these are clearly an essential tool for studying the decomposition chemistry of nitramine propellants, but mass spectroscopy suffers somewhat as a detection technique from the fact that missing mass peaks, unexpected cracking patterns, complex TOF patterns, and lack of structural information on the products sometimes leads to uncertainties in the interpretation of the identification of the molecular species. It is precisely these uncertainties which might be resolved by microwave studies of the type described here.

## II. Experimental Results

The instruments employed are (a) a Stark-modulated millimeterwave spectrometer with computer controlled frequency scanning and equipped with a pyrolysis source, and (b) pulsed-beam Fabry-Perot cavity Fourier-transform microwave (FTMW) spectrometer with a heated nozzle source<sup>19</sup> shown in Figure 1. The frequency coverage of the millimeterwave spectrometer (a) is 18 GHz to 170 GHz using both solid-state and klystron frequency sources, while for the FTMW spectrometer (b) the current frequency range is 6 GHz to 26 GHz. Both spectrometers have computer controlled scan capabilities for broad-band coverage. In the millimeterwave study we used a flow pyrolysis system consisting of a 6 mm o.d. glass tube, filled with granular zeolite material (alumina-silicate) which has been found to produce pyrolytic decomposition at reduced temperatures, heated to 200°-450° C over a length of about 20 cm to study the thermal decomposition products of RDX vapor.

The RDX solid was placed in a small quartz boat 10 cm in length and heated to between 140° and 150° C by a heating tape wrapped around the glass tube surrounding the RDX sample. This system is illustrated in Figure 2a. and 2b.

## 1. Pulsed-beam Fourier-Transform Experiments

### A. Survey of RDX

We have covered the frequency range searched for decomposition products with the FTMW spectrometer with coverage of 6.6 GHz between 8-18 GHz. The RDX sample was placed in a heated reservoir of the pulsed nozzle and pressurized with Ar at 1.2 kPa. Most of the survey was carried out with nozzle temperatures between 140°C and 150°C, and covered the key regions of the known decomposition products as well as searches for methylene nitramine,  $\text{CH}_2=\text{NNO}_2$ , which is produced in the unimolecular decomposition by Zhao, *et al.*<sup>1</sup>. By far the most intense products are  $\text{H}_2\text{CO}$  and  $\text{N}_2\text{O}$ , followed by  $\text{HONO}$ ,  $\text{NH}_2\text{CHO}$  (formamide) and  $\text{HNCO}$ . In addition to monomer spectra, several dimers were observed, namely  $(\text{H}_2\text{O})_2$ , Ar- $\text{H}_2\text{CO}$ , and  $\text{NH}_2\text{CHO}-\text{H}_2\text{O}$ , since the beam temperature is between 1-5 K. The water appears to originate in the decomposition, since it is not "baked out" of the sample. The species  $\text{H}_2\text{CO}$ ,  $\text{N}_2\text{O}$ , and  $\text{NH}_2\text{CHO}$  were sufficiently intense to allow measurement over a range in temperatures (about 140°-190°C) and each showed an exponential growth since the vapor pressure and decomposition are proportional to the temperature. Only one feature has been observed but not assigned. This occurs as a triplet near 9156.35 MHz, the carrier contains  $\text{H}_2\text{CO}$  since it is observed from a pure formaldehyde sample. A summary of the transitions detected in this survey is given in Table I. No

evidence was found for spectra from RDX or methylene nitramine.

### B. Structure of Nitromethane-Water

The stimulus for the study of the nitromethane-water complex derives from the theoretical work of Melius<sup>20,21</sup> in which water is found to exert a strong catalytic effect in reducing the barrier to the decomposition of nitramines. Examples are presented for the reactions of nitramine and nitromethane in which "water provides a concerted, cyclic reaction pathway for reduction of the nitro group."<sup>21</sup> The transition state, depicted in Fig. 1b, shows a reduction in the barriers by 27 kcal mol<sup>-1</sup>. We have studied a number of complexes in which the transition state geometry is replicated by the van der Waals complex at longer distance and strongly suggest that the complexes lie along the reaction coordinate. Examples studied are the complexes for ozone-ethylene<sup>22</sup>, ozone-acetylene<sup>23</sup> and ketene-ethylene<sup>24</sup>; the ozone complexes exhibit cyclic van der Waals structures and ketene-ethylene has the heavy atom frames crossed at 90°. Thus, we were interested in determining the geometry the nitromethane-water with respect to the proposed cyclic transition state. The microwave spectrum of the nitromethane-water complex has been studied with FTMW spectrometer. The dominant spectrum is *b*-type with a weaker *a*-type spectrum. Critical to the rotational assignments were well resolved <sup>14</sup>N nuclear electric quadrupole transitions, and the incorporation of the pulsed nozzle in one of the mirrors which provided a beam co-axial with the cavity axis to attain linewidths on the order of 2 kHz. In addition to the CH<sub>3</sub>NO<sub>2</sub>-H<sub>2</sub>O species, substitutions of HDO and D<sub>2</sub>O in the complex were made, and the CD<sub>3</sub>NO<sub>2</sub>-H<sub>2</sub>O species was also assigned. The molecular structure derived from the moments of

inertia, shown in Fig. 3, has the dipolar axes of each monomer nearly parallel with a center of mass separation of 3.506(7) Å. The complex is quite strongly bonded with a stretching force constant  $k_s = 9.3$  N/m and evidence for two hydrogen bonds of 2.16 Å between an O atom of the  $\text{NO}_2$  group and a water H atom, and 2.09 Å between a  $\text{CH}_3$  proton and the oxygen atom of water. Unpublished *Ab initio* calculations by W. J. Stevens support this structure. A report describing these results has been accepted for publication in *J. Mol. Spectrosc.*<sup>25</sup>

## 2. Pyrolysis Studies of RDX Vapor - Microwave Studies

This experiment involves a conventional microwave absorption spectrometer equipped with a pyrolysis inlet. The RDX sample is heated to a fixed temperature, typically 145° C, and the vapor passes over an alumina-silica catalyst at a higher temperature (200°-450° C) to decompose the vapor. Extensive surveys have been conducted between 54 GHz and 150 GHz with a new synthesizer-locked backwardwave oscillator source from 50-78 GHz and 78-118 GHz from the Russian firm Kvarz. We were able to frequency double the lower frequency unit to survey the region from 123.5-150 GHz. We have assigned less than 10% of these transitions to known species. As in the nozzle experiment, the dominant products are  $\text{H}_2\text{CO}$  and  $\text{N}_2\text{O}$ , with ground and vibrationally excited states detected. Formamide ( $\text{NH}_2\text{CHO}$ ) and isocyanic acid (HNCO) are observed and the latter peaks at high catalyst temperature (about 400° C), which suggests that HNCO is produced by decomposition of another product, perhaps formamide, produced at an earlier stage. Several transitions of  $\text{NO}$ ,  $\text{NO}_2$  and  $\text{HONO}$  are observed but are quite weak. The new survey also show more than a dozen lines of  $\text{CH}_3\text{OH}$ . The methanol appears to be an impurity in the RDX sample

since its spectra grows weak the longer the RDX sample is heated, while the other products continue to show strong spectral lines. Our survey contains hundreds unidentified features, and efforts to assign these (or a subgroup of these) to the triple fission product,  $\text{CH}_2=\text{NNO}_2$ , were unsuccessful in spite of a high quality *ab initio* structure as a guide. Figure 4 shows a calculated spectrum of  $\text{CH}_2=\text{NNO}_2$  based on the *ab initio* structure<sup>26</sup> between 75 GHz and 120 GHz; this may be compared to the observed unassigned spectra over the same frequency range in Figure 4. Thus, either  $\text{CH}_2=\text{NNO}_2$  is not produced in the RDX vapor decomposition or it is not sufficiently stable to be detected under the conditions of this experiment. A summary of the observed microwave transition for the species identified is given in Table II and the unassigned lines are listed in Appendix I. Behrens and Bulusu<sup>14</sup> report N-methylformamide,  $\text{CH}_3\text{NHCHO}$  (mass 59), as a minor product based on the ion signal at  $m/z = 58$ . We have examined and assigned a portion of the millimeterwave spectrum of N-methylformamide with the aid of unpublished lower frequency measurements by R. A. Elzara (PhD Thesis Michigan State University). When comparing the same spectral region surveyed in the RDX pyrolysis, no evidence of N-methylformamide was found.

#### A. Species X - Assignment of Unidentified Species

During the course of surveying the pyrolysis products of RDX vapor, three lines with resolved Stark effect were observed between 70 GHz and 75 GHz. Each had two Stark shifted components characteristic of *a*-type  $J = 2-1$  R-branch transitions. Subsequent scans at higher harmonic frequencies for the  $J = 3-2$  and  $J = 4-3$  transitions provided additional transitions with the expected Stark effect for this assignment. Table IV lists 12 assigned

transitions for this unknown molecular species which we have labeled "Species-X". The fitted rotational constants are also shown in Table IV. We have tested Species-X by applying a strong magnetic field and see no effect on the spectral lines, thus, it is not paramagnetic and eliminates a radical as a source of the spectrum. The inertial defect,  $\Delta I$ , is small and positive, which indicates that Species-X is a planar molecule. The magnitude of the rotational constants indicates the species is light and prolate (like formaldehyde or methanol) and the assigned lines all arise from a  $\mu_a$  dipole moment component. We attempted to locate a *b*-type or *c*-type Q-branch series unsuccessfully. Species-X was observed from virtually every sample of RDX which we pyrolyzed, and also was observed in several sample of HMX pyrolyzed in the same manner as the RDX experiment. Assuming that Species-X is a product of RDX vapor decomposition, and there is no reason to believe otherwise, it is constrained to be composed of  $H_n C_x N_y O_z$  where n, x, y, and z are integers, since the empirical formula of RDX is  $C_3 H_6 N_6 O_6$ . Further, every known species having three first row atoms (C, N or O) in any combination has B and C rotational constants near 10 to 13 GHz, much smaller than Species-X. Thus, we are led to believe that Species-X can contain only two of these first row atoms. In Table V we have constructed a chart of all pairs of C, N, and O and then adding H's until the valence bonding is saturated. At the bottom of Table V rotational constants from microwave spectral analysis are shown. From the magnitude of the A rotational constant (140 GHz) for Species-X, it is clear that 3 hydrogen atoms off the heavy atom axis ( $H_2 NOH$  or  $CH_2 = NH$ ) are too few and 5 hydrogen atoms are too many ( $CH_3 NH_2$ ), while 4 hydrogen atoms are close ( $H_2 N NH_2$  and  $CH_3 OH$ ). The methylamine B and C rotational constants are slightly larger (10%) than Species-X, which is true of the

other saturated forms of the diatoms. The puzzle is in the fact that all of the stable species (radicals were not considered based on the results of the paramagnetic test) we can conceive of are listed in Table V and each of these either has no microwave spectrum ( $H_nC_2$  species) due to a lack of dipole moment, or has already been assigned, i.e. we know the rotational constants, and these do not explain Species-X. Thus, our best guess for the formula of Species-X is  $H_4XY$ , where X and Y = C, N, or O.

#### B. Temperature profiles

Temperature profiles of the identified species whose intensities were sufficiently strong were measured by keeping the temperature of the RDX sample constant and increasing (or decreasing) the temperature of the catalyst pyrolysis zone. In Figure 6 profiles for HCN,  $H_2CO$ ,  $N_2O$ , CO, HNCO, and Species-X are shown. The results are rather poor due to the slow flow employed in order to maintain a constant pressure in the absorption cell. With increasing temperature the cell pressure increased due to more decomposition, while the opposite occurs when starting at the highest temperature and decreasing the temperature. However, a general trend is evident: The  $N_2O$ ,  $H_2CO$  and Species-X were strongest at pyrolysis temperatures between 250° C and 300° C, while HCN and HNCO had a peak intensity between 400° C and 450° C. The CO species was rather constant over the whole range and  $NO_2$  shows increasing intensity up to 450° C. Thus, it would appear that Species-X,  $H_2CO$  and  $N_2O$  appear as first stage products, while HCN and HNCO are second stage products, i.e. result from pyrolysis of first stage products. Very likely HNCO comes from pyrolysis of formamide ( $NH_2CHO$ ). These results are in agreement with those of Behrens and Bulusu<sup>14</sup>. It is interesting that species-X correlates with the first stage products.

### III. Conclusions

The unimolecular laser infrared multiphoton dissociation (IRMPD) photolysis decomposition scheme for RDX proposed by Zhao, et al.<sup>1</sup> showed that the dominant channel is a concerted triple fission of the RDX ring to produce three  $\text{CH}_2\text{N}_2\text{O}_2$  (mass 74) fragments and identified it to be the  $\text{CH}_2=\text{NNO}_2$  species. Behrens and Bulusu<sup>2</sup> have studied the decomposition of liquid RDX and several isotopically labeled species and concluded that four pathways occur in the liquid including a surface catalyzed path in which  $\text{NH}_2\text{CHO}$  is produced. Several large species were initially formed, namely, oxy-s-triazine ( $\text{C}_3\text{H}_3\text{N}_3\text{O}$ ) and 1-nitroso-3,3-dinitrohexahydro-s-triazine, whose structure and microwave spectra are unknown. The observed products in our experiments correlate better with the mechanism of Behrens and Bulusu, although several differences were found. We did not observe N-methylformamide attributed to mass peak  $m/z = 58$ , and we detected several species not reported in the mass spectrometry study, namely, Species-X,  $\text{HCOOH}$ ,  $\text{HNCO}$ , and possibly acetaldehyde,  $\text{CH}_3\text{CHO}$ . Most of the spectral lines observed in the millimeterwave survey remain unassigned. Perhaps these may be attributed to the two species detected by mass spectrometry, OST (oxy-s-triazine) and ONDNTA (1-nitroso-3,5-dinitrohexahydro-s-triazine), whose microwave spectrum is unknown. Cosgrove and Owen<sup>27</sup> reported the detection of formic acid in the decomposition of RDX vapor at  $195^\circ \text{C}$  via a chemical test. It might be noted that  $\text{HCOOH}$  has the same mass (46) as  $\text{NO}_2$  and  $\text{CH}_3\text{CHO}$  has the same mass (44) as  $\text{N}_2\text{O}$ , thus, the presence in the mass spectrum might be masked by this other known products.

## REFERENCES

1. T. L. Boggs, "The Thermal Behavior of Cyclotrimethylene-trinitramine(RDX) and Cyclotetramethylene-tetranitramine (HMX)," in Fundamentals of Solid-Propellant Combustion, K. K. Kuo and M. Summerfield, Eds., Prog. in Aeronautics and Astronautics **90**, 121 (1984).
2. R. A. Fifer, "Chemistry of Nitrate Ester and Nitramine Propellants," in Fundamentals of Solid-Propellant Combustion, K. K. Kuo and M. Summerfield, Eds., Prog. in Aeronautics and Astronautics **90**, 177 (1984).
3. M. A. Schroeder, "Critical Analysis of Nitramine Decomposition Data: Activation Energies and Frequency Factors for HMX and RDX Decomposition," Report No. BRL-TR-2673, Ballistics Research Laboratory, Aberdeen Proving Ground, Aberdeen, Maryland MD (September 1985); M. A. Schroeder, "Critical Analysis of Nitramine Decomposition Data: Product Distributions from HMX and RDX Decomposition," Report No. BRL-TR-2659 (June 1985).
4. M. D. Cook, *J. Energ. Materials* **5**, 257 (1987).
5. B. Suryanarayana, R. Graybush, and J. R. Autera, *Chem. and Ind.* 2177 (1967).
6. F. I. Dubovitskii and B. L. Korsunski, *Russian Chem. Rev.* **50**, 958-978 (1980) [*Uspeki Khimii* **50**, 1828-1871 (1981)].
7. R. W. Shaw, Jr. and G. F. Adams, Eds, "Diagnostics for Propellant Ignition," Army Research Office (June 1985), DTIC No. B093719.
8. C. F. Melius, "Thermochemical Modeling: I. Application to Decomposition of Energetic Materials," in Chemistry and Physics of Energetic Materials, S. N. Bulusu, ed., Kluwer Academic Publishers, Dordrecht, The Netherlands, p21-49 (1990).
9. C. F. Melius, "Thermochemical Modeling: II. Application to Ignition and Combustion of Energetic Materials," in Chemistry and Physics of Energetic Materials, S. N. Bulusu, ed., Kluwer Academic Publishers, Dordrecht, The Netherlands, p51-78 (1990).
10. R. Hatch, "Chemical Kinetics Modeling of HMX Combustion," presented at the 24th JANNAF Combustion Meeting, Monterey Calif. (1987).
11. X. Zhao, E. J. Hintsza and Y. T. Lee, "Infrared multiphoton dissociation of RDX in a molecular beam," *J. Chem. Phys.* **88**, 801 (1988).
12. R. Behrens, "The Application of Simultaneous Thermogravometric Modulated Beam

Mass Spectrometry and Time-of-Flight Velocity Spectra Measurements to the Study of the Pyrolysis of Energetic Materials," in Chemistry and Physics of Energetic Materials, S. N. Bulusu, ed., p327-346.

13. R. Behrens, "Thermal Decomposition of HMX and RDX: Decomposition Processes and Mechanisms Based on STMBMS and TOF Velocity-spectra Measurements," in Chemistry and Physics of Energetic Materials, S. N. Bulusu, ed., p347-368.
14. R. Behrens, Jr., and S. Bulusu, "Thermal Decomposition of Energetic Materials. 3. Temporal Behaviors of the Rates of Formation of the Gaseous Pyrolysis Products from Condensed-Phase Decomposition of 1,3,5-Trinitrohexahydro-s-triazine," *J. Phys. Chem.* **96**, 8877 (1992).
15. R. Behrens, Jr., and S. Bulusu, "Thermal Decomposition of Energetic Materials. 4. Deuterium Isotope Effects and Isotopic Scrambling (H/D,  $^{13}\text{C}/^{18}\text{O}$ ,  $^{14}\text{N}/^{15}\text{N}$  in Condensed-Phase Decomposition of 1,3,5-Trinitrohexahydro-s-triazine," *J. Phys. Chem.* **96**, 8891 (1992).
16. F. J. Lovas, F. O. Clark and E. Tiemann, "Pyrolysis of Ethylamine. I. Microwave Spectrum and Molecular Constants of Vinylamine," *J. Chem. Phys.* **62**, 1925 (1975).
17. F. J. Lovas, R. D. Suenram, D. R. Johnson, F. O. Clark and E. Tiemann, "Pyrolysis of Ethylamine II. Synthesis and Microwave Spectrum of Ethylenimine ( $\text{CH}_3\text{CH}=\text{NH}$ )," *J. Chem. Phys.* **72**, 4964 (1980).
18. F. J. Lovas, "Application of Microwave Spectroscopy to Chemical Analysis," *ISA Transactions* **14**, 145 (1975).
19. F. J. Lovas, and R. D. Suenram, "Pulsed Beam Fourier Transform Microwave Measurements on OCS and Rare Gas Complexes of OCS with Ne, Ar, and Kr," *J. Chem. Phys.* **87**, 2010 (1987); R. D. Suenram, F. J. Lovas, G. T. Fraser, J. Z. Gillies, C. W. Gillies, and M. Onda, "Microwave Spectrum, Structure, and Electric Dipole Moment of Ar- $\text{CH}_3\text{OH}$ ," *J. Mol. Spectrosc.* **137**, 127 (1989).
20. C. F. Melius, in Chemistry and Physics of Energetic Materials (ed. S. Bulusu), pp. ASI 309, NATO.
21. C. A. Melius, *Phil. Trans. R. Soc. Lond. A* **339**, 365-376 (1992).
22. J. Z. Gillies, C. W. Gillies, R. D. Suenram, F. J. Lovas, and W. Stahl, *J. Amer. Chem. Soc.* **111**, 3073-3074 (1989); C. W. Gillies and J. Z. Gillies, R. D. Suenram, F. J. Lovas, E. Kraka, and D. Cremer, *J. Am. Chem. Soc.* **113**, 2412-2421 (1991).
23. J. Z. Gillies, C. W. Gillies, F. J. Lovas, K. Matsumura, R. D. Suenram, E. Kraka,

and D. Cremer, *J. Am. Chem. Soc.* **113**, 6408-6415 (1991).

24. C.W. Gillies, J.Z. Gillies, F.J. Lovas, and R.D. Suenram, *J. Am. Chem. Soc.* **115**, 9253-62 (1993).

25. F.J. Lovas, N. Zobov, G.T. Fraser, and R.D. Suenram, *J. Mol. Spectrosc.* **171**, xxx (1995).

26. R.C. Mowrey, M. Page, G.F. Adams, and B.H. Lengsfield III, *J. Chem. Phys.* **93**, 1857 (1990).

27. J.D. Cosgrove and A.J. Owen, *Combustion and Flame* **22**, 13 (1974).

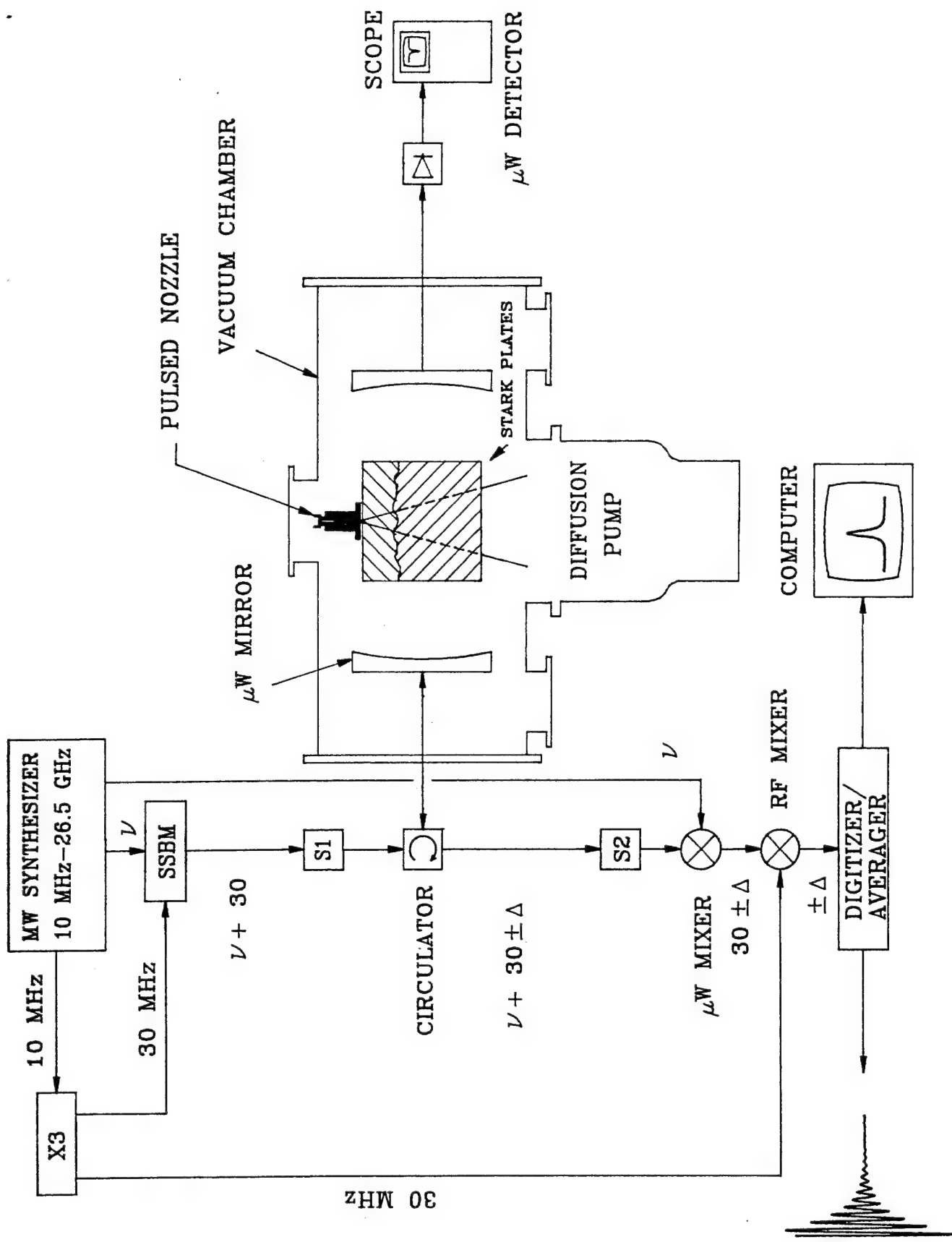
## LIST OF PUBLICATIONS

F.J. Lovas, N. Zobov, G.T. Fraser, and R.D. Suenram, *J. Mol. Spectrosc.* **171**, xxx (1995).

## LIST OF PARTICIPATING SCIENTIFIC PERSONNEL

N. Zobov, NIST Guest Worker  
M-Yu. Tretyakov, NIST Guest Worker  
Institute of Applied Physics  
Nizhny Novgorod, Russia

G.T. Fraser, NIST staff



## Millimeterwave Synthesizer

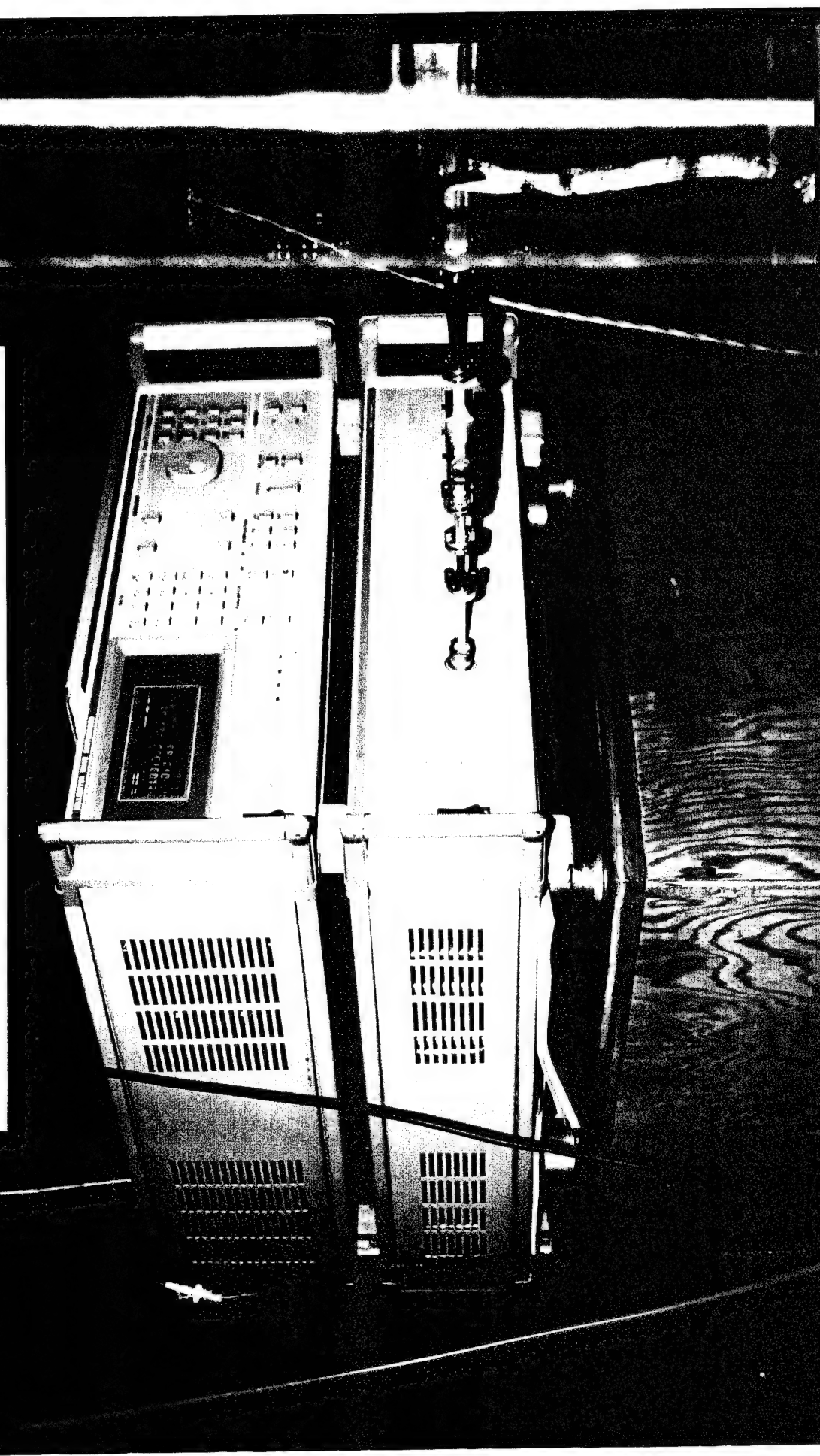


Fig. 2a.

# Pyrolysis Oven

Sublimation  
Region

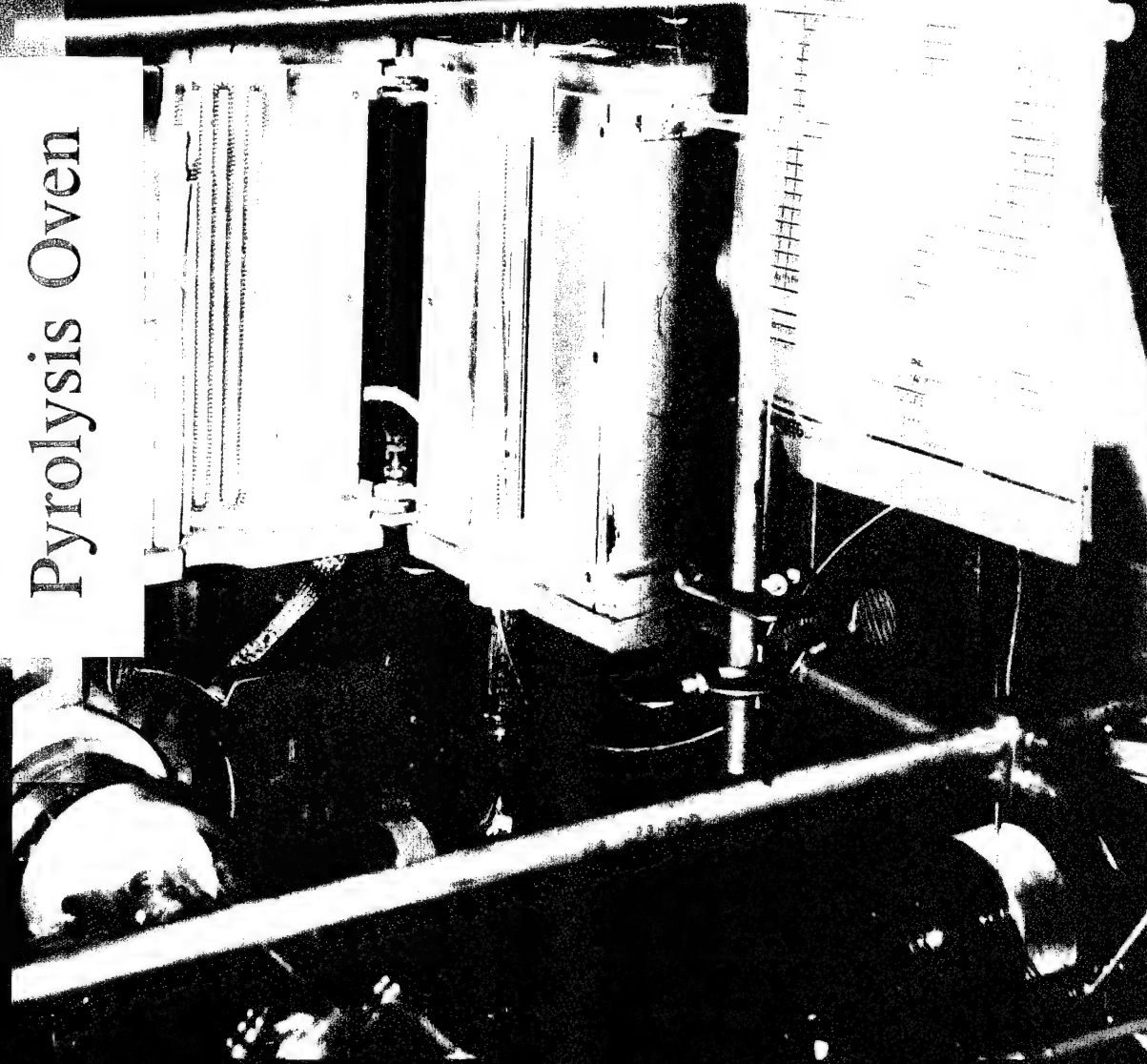
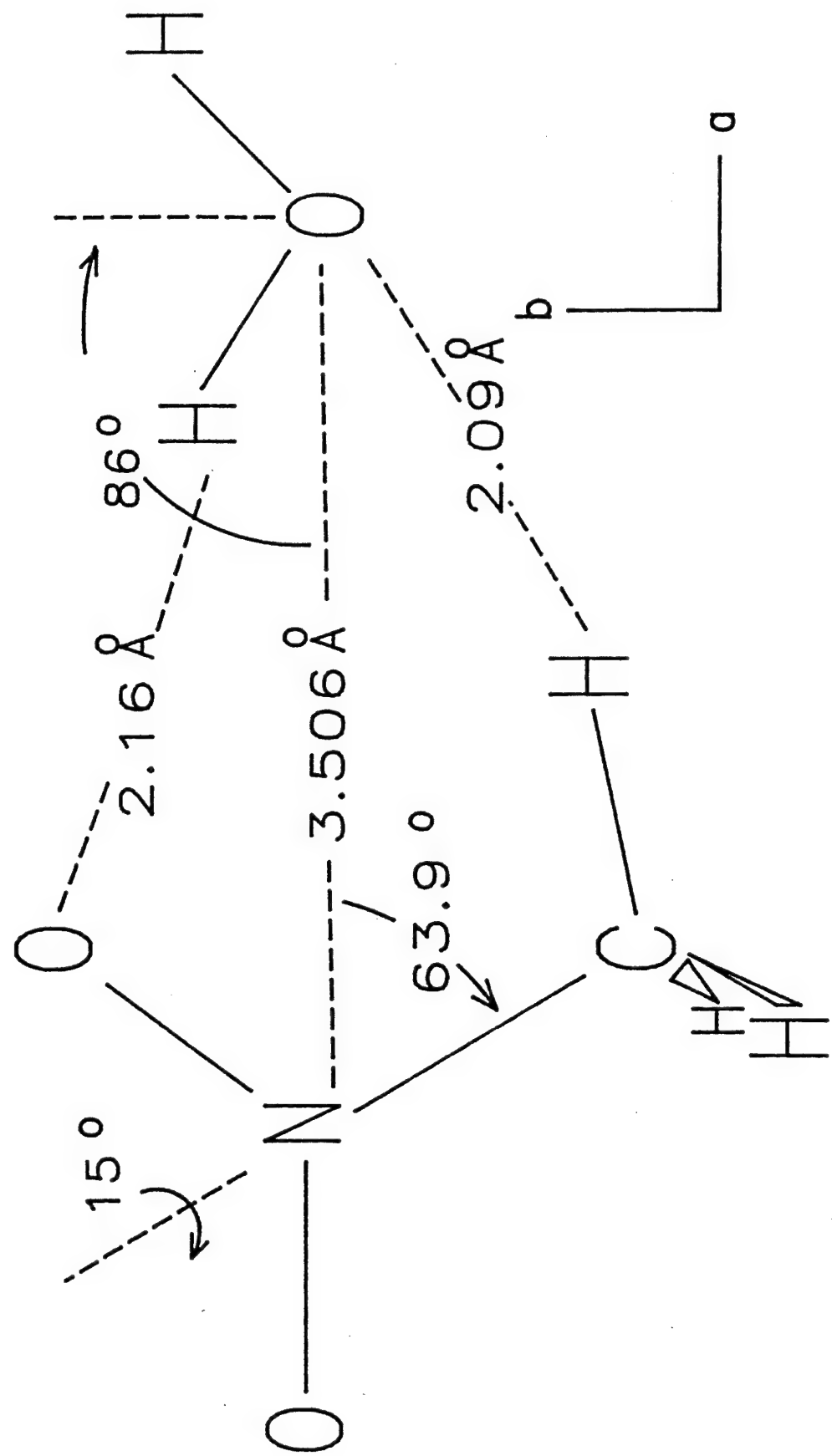
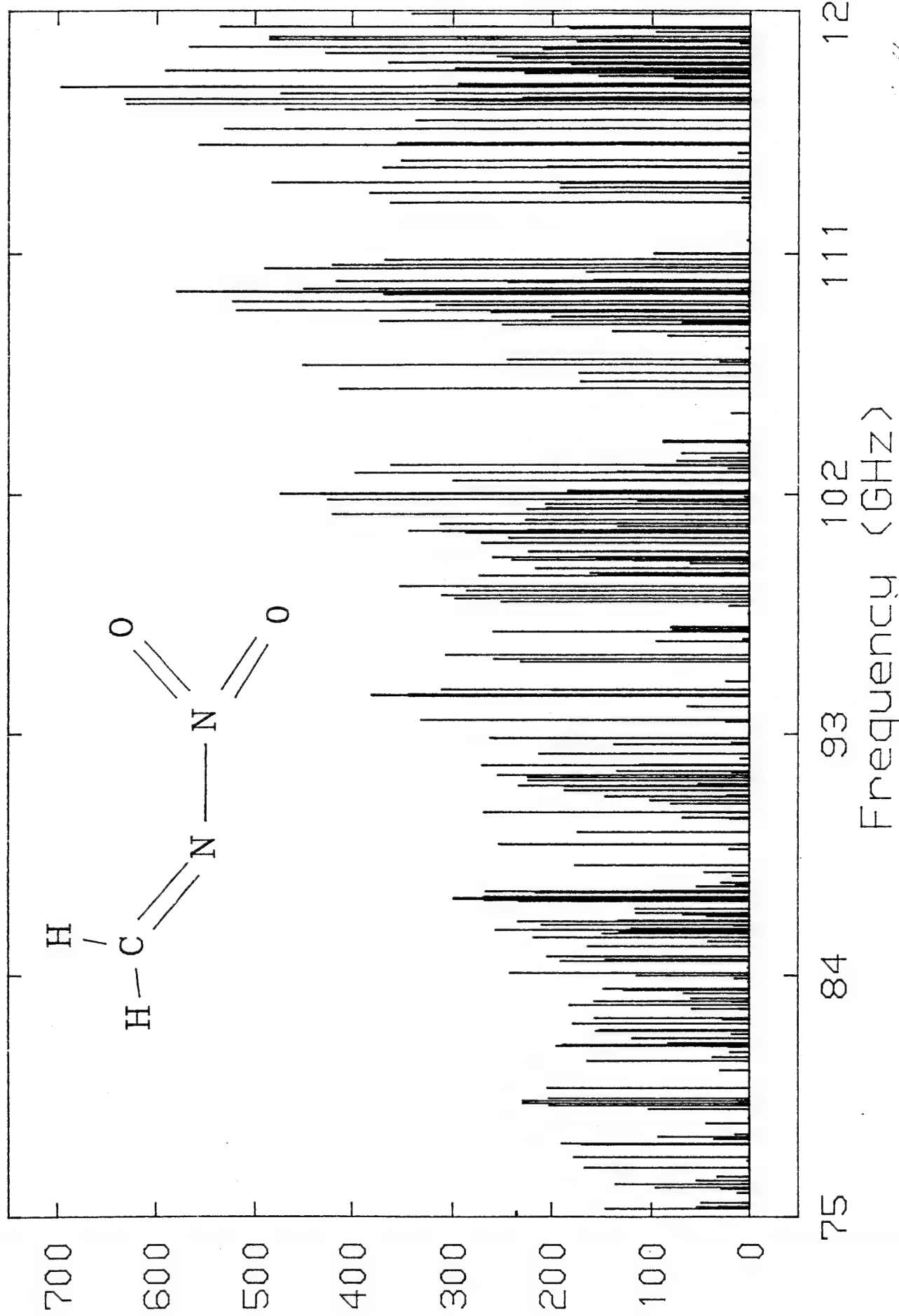
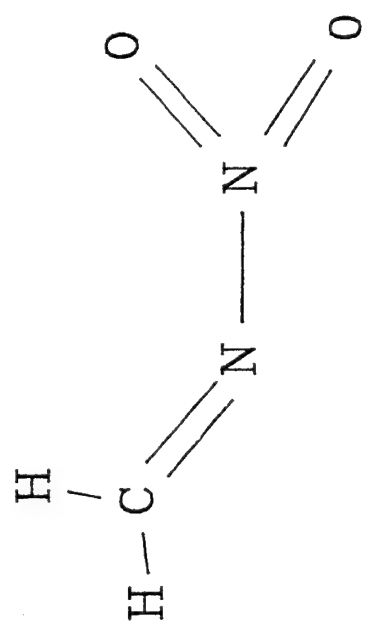


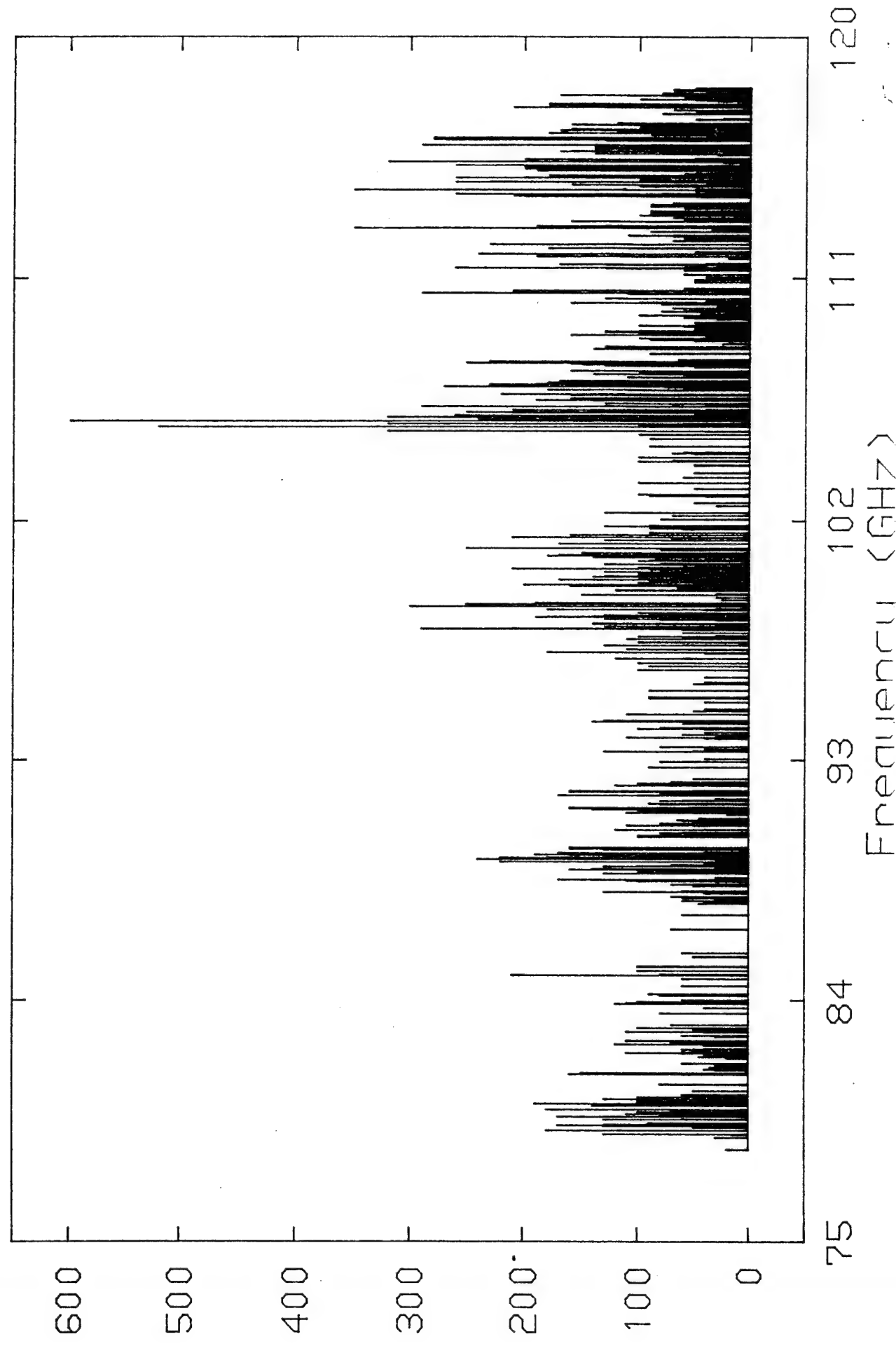
Fig. 2b.



Calculated



Observed



# RDX Pyrolysis Products

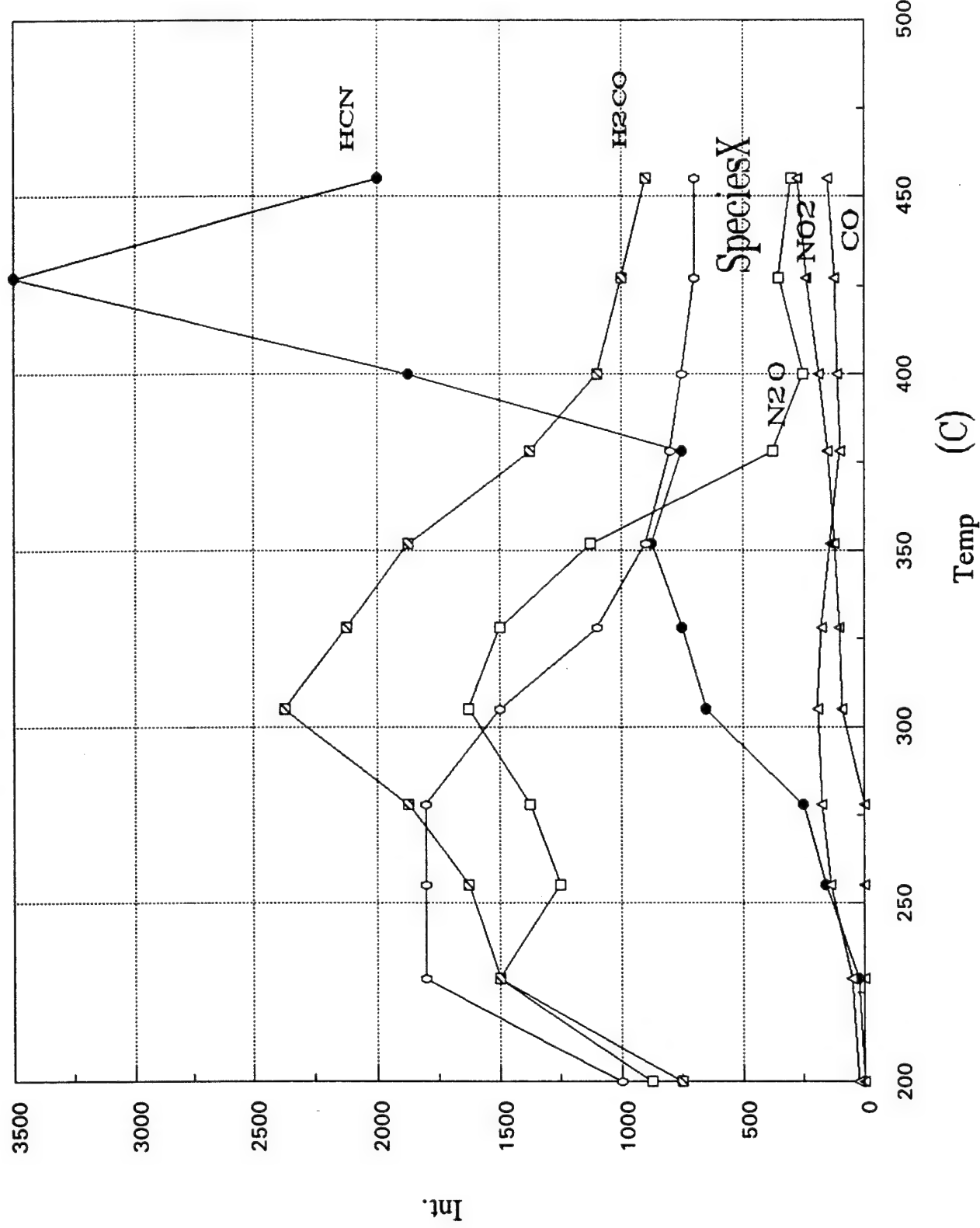


Fig. 6

TABLE I. Microwave Transitions Identified in Heated Nozzle FTMW Study of RDX

Frequency	Species	Transition	Comments
14488.47	H <sub>2</sub> CO	2(1,1) -2(1,2)	S/N = 30
25123.30	N <sub>2</sub> O	1 - 0	S/N = 40
23541.491	HONO	1(0,1) - 0(0,0)	S/N = 0.21
21982.097	HNCO	1(0,1) - 0(0,0)	S/N = 0.13
9237.027	NH <sub>2</sub> CHO	3(1,2) - 3(1,3)	S/N = 0.13
15392.501	NH <sub>2</sub> CHO	4(1,3) - 4(1,4)	S/N = 0.5
21207.234	NH <sub>2</sub> CHO	1(0,1) - 0(0,0)	S/N = 0.7

TABLE II. Microwave Transitions Identified in Pyrolysis MW Study of RDX

Frequency	Species	Transition
66973.496	H <sub>2</sub> CO	12(2,10)-12(2,11)
72409.097	H <sub>2</sub> CO	1(0,1) - 0(0,0)
72838.948	H <sub>2</sub> CO	5(1,4) - 5(1,5)
78230.50	H <sub>2</sub> CO	21(3,18)-21(3,19)
116718.615	H <sub>2</sub> CO	14(2,12)-14(2,13)
127154.96	H <sub>2</sub> CO	23(3,20)-23(3,21)
145389.34	H <sub>2</sub> CO	v <sub>5</sub>
145603.64	H <sub>2</sub> CO	2(02) - 1(01)
146635.3	H <sub>2</sub> <sup>13</sup> CO	2(02) - 1(01)
150400.72	H <sub>2</sub> CO	v <sub>5</sub>
75369.22	N <sub>2</sub> O	3 - 2
125613.92	N <sub>2</sub> O	5 - 4
125663.52	N <sub>2</sub> O	5 - 4
125901.28	N <sub>2</sub> O	5 - 4
125948.00	N <sub>2</sub> O	5 - 4
125948.96	N <sub>2</sub> O	5 - 4
53721.74	HCN	15 - 15
60861.65	HCN	16 - 16
68441.92	HCN	17 - 17
76461.46	HCN	18 - 18
84919.16	HCN	19 - 19
88630.416	HCN	1 - 0 F = 1 - 1
88631.847	HCN	1 - 0 F = 2 - 1
88633.936	HCN	1 - 0 F = 0 - 1
93813.84	HCN	20 - 20
103144.25	HCN	21 - 21
112909.10	HCN	22 - 22
65699.74	HNCO	3(1,3) - 2(1,2)
65946.17	HNCO	3(0,3) - 2(0,2)
65181.97	HNCO	3(1,2) - 2(1,1)
109498.34	HNCO	5(1,5) - 4(1,4)
109833.	HNCO	5(3 ) - 4(3 )
109875.8	HNCO	5(2 ) - 4(2 )
109908.95	HNCO	5(0,5) - 4(0,4)
109959.	HNCO	33(1,33) - 34(0,34)
113736.30	HNCO	43(0,43) - 42(1,42)
70588.6	NO <sub>2</sub>	7(1,1) - 8(0,8)
70646.2	NO <sub>2</sub>	7(1,1) - 8(0,8)
70654.1	NO <sub>2</sub>	7(1,1) - 8(0,8)
150439.22	NO	3/2,3/2-1/2,3/2

TABLE II. Microwave Transitions Identified in Pyrolysis MW Study of RDX  
(CONTINUED)

Frequency	Species	Transition
109753.59	NH <sub>2</sub> CHO	5(1,4) - 4(1,3)
127112.854	NH <sub>2</sub> CHO	6(2,5) - 5(2,4)
127330.361	NH <sub>2</sub> CHO	6(5 ) - 5(5 )
127348.704	NH <sub>2</sub> CHO	6(4 ) - 5(4 )
127393.783	NH <sub>2</sub> CHO	6(3,4) - 5(3,3)
127412.357	NH <sub>2</sub> CHO	6(3,3) - 5(3,2)
128102.967	NH <sub>2</sub> CHO	6(2,4) - 5(2,3)
148223.377	NH <sub>2</sub> CHO	7(2,6) - 6(2,5)
148556.391	NH <sub>2</sub> CHO	7(6 ) - 6(6 )
148567.324	NH <sub>2</sub> CHO	7(5 ) - 6(5 )
148599.5	NH <sub>2</sub> CHO	7(4 ) - 6(4 )
148667.617	NH <sub>2</sub> CHO	7(3,5) - 6(3,4)
148709.342	NH <sub>2</sub> CHO	7(3,4) - 6(3,3)
149792.812	NH <sub>2</sub> CHO	7(2,5) - 6(2,4)
98087.42	HONO	6(1,5) - 6(0,6)
104237.45	HONO	7(1,6) - 7(0,7)
111551.60	HONO	8(1,7) - 8(0,8)
113841.170	HONO	5(1,5) - 4(1,4)
117281.36	HONO	5(0,5) - 4(0,4)
115271.207	CO	1 - 0
112287.11	HCOOH	5(2,4 - 4(2,30
112432.40	HCOOH	5(4) - 4(4)
112459.72	HCOOH	5(3,3) - 4(3,2)
112466.92	HCOOH	5(3,2) - 4(3,1)
112254.80	CH <sub>3</sub> CHO	6(1,6) - 5(1,5) E

TABLE III. Species Identified by Mass Spectrometry and Microwave Spectroscopy

	Mass Spectrometry <sup>1</sup>	This Work
H <sub>2</sub> O	yes	no line in range
HCN	yes	yes
CO	yes	yes
H <sub>2</sub> CO	yes	yes
NO	yes	yes
N <sub>2</sub> O	yes	yes
NO <sub>2</sub>	yes	yes
HNCO	NO	yes
HONO	yes	yes
NH <sub>2</sub> CHO	yes	yes
CH <sub>3</sub> NHCHO	yes	NO
oxy- <i>s</i> -triazine	yes	spectrum unknown
ONDNTA <sup>2</sup>	yes	spectrum unknown
HCOOH	NO	yes
CH <sub>3</sub> CHO	NO	yes?

1. Behrens & Bulusu, JPC **96**, 8877-8891 (1992).

2. 1-Nitroso-3,5-dinitrohexahydro-*s*-triazine

TABLE IV. Species X Rotational Parameters

Quantum Numbers	Observed Transitions		Rotational Parameters	
	Obs. Freq. <sup>a</sup>	Obs.-Calc. <sup>a</sup>	Constant	Value <sup>a</sup>
2 <sub>12</sub> -1 <sub>11</sub>	70419.817	0.012	A (MHz)	141019.58
2 <sub>02</sub> -1 <sub>01</sub>	72801.475	-0.002	B (MHz)	19417.002(13)
2 <sub>11</sub> -1 <sub>10</sub>	75249.200	-0.003	C (MHz)	17002.124(12)
3 <sub>13</sub> -2 <sub>12</sub>	105605.596	-0.170	Δ <sub>JK</sub> (kHz)	645.3(44)
3 <sub>03</sub> -2 <sub>02</sub>	109111.140	0.066	Δ <sub>J</sub> (kHz)	36.43(43)
3 <sub>22</sub> -2 <sub>21</sub>	109238.000	0.047	δ <sub>J</sub> (kHz)	5.60(34)
3 <sub>12</sub> -2 <sub>11</sub>	112848.900	0.038	ΔI (uÅ <sup>2</sup> )	0.113
4 <sub>14</sub> -3 <sub>13</sub>	140763.310	-0.155		
4 <sub>04</sub> -3 <sub>03</sub>	145311.620	-0.023		
4 <sub>23</sub> -3 <sub>22</sub>	145618.800	-0.033		
4 <sub>13</sub> -3 <sub>12</sub>	150418.140	0.000		
5 <sub>15</sub> -4 <sub>14</sub>	175884.350	0.099		

a. In MHz

TABLE V. Candidate molecular sources for Species-X

CC	CN	CO	NN	NO	OO
HCCH	HCN	HCO	HNN	HNO	HOOH
$\text{CH}_2=\text{CH}_2$	$\text{CH}_2=\text{NH}$	$\text{H}_2\text{CO}$	$\text{H}_2\text{NNH}_2$	$\text{H}_2\text{NOH}$	
$\text{CH}_3\text{CH}_3$	$\text{CH}_3\text{NH}_2$	$\text{CH}_3\text{OH}$			
Species	A (GHz)	B (GHz)	C (GHz)		
<b>Species-X</b>	<b>141.0</b>	<b>19.42</b>	<b>17.00</b>		
$\text{CH}_2=\text{NH}$	196.2	34.6	29.3		
$\text{CH}_3\text{NH}_2$	103.1	22.63	21.71		
$\text{H}_2\text{CO}$	281.9	38.8	34.0		
$\text{CH}_3\text{OH}$	127.6	24.69	23.78		
$\text{H}_2\text{NNH}_2$	143.4	24.08	24.07		
$\text{H}_2\text{NOH}$	190.9	25.2	25.1		
HNCO	918.5	11.07	10.9		

APPENDIX 1. Spectral Line Survey of RDX Decomposition Products

Frequency	Intensity (μV)				
53 721.630	300	very slow +	70 754.000	50	
53 852	30		70 760.600	50	
53 962	30		71 650.800	30	
54 062	30		71 669.220	70	
54 097	40		71 684.200	50	
54 207	30		72 801.740	260	slow + -
54 310	40		75 249.190	900	very slow - slow +
54 403	40	slow +	76 461.350	200	very slow +
54 931	30		78 437	20	
59 342.340	40		78 876.930	30	+
59 929	30		78 978	15	
59 947	30		79 004.820	130	
60 285	30	slow +	79 135.980	180	
60 612	50		79 232.700	30 \	
60 861.600	260	very slow +	79 234.460	50 /	
65 232	30	-	79 249.160	30	
65 653	70		79 298.420	130	
65 880	40	-	79 338.570	170	broad
66 083	30		79 363.260	130	+
66 249	30		79 408.180	90	
67 033	30	-	79 411.980	70	
67 218	70	+	79 544.080	130	
67 275	30		79 560.760	60	
67 833	40		79 652.380	130	
67 893	60		79 656.420	170	
68 286	30		79 720.200	80	
68 441.800	230	very slow +	79 744	25	?
68 634	50	slow +	79 751.250	110	broad
68 752	60	slow +	79 779.380	30	
68 908	30		79 789.560	100	broad
69 384	40		79 795.860	60	+
69 411	50	slow -	79 835.840	100	
69 442	40		79 852.120	70	
69 555	50		79 885.700	30	
69 613	50		79 917.480	180	
69 628	40		80 054.580	140	
70 364.640	30		80 116.540	130	
70 385.600	40		80 140.800	190	-
70 419.800	500	very slow - slow +	80 169.450	100	
70 429.800	30		80 181.980	80	
70 603.300	30		80 190.740	30	slow -
70 605.900	30		80 208.620	60	
70 620.700	40		80 220.020	50	
70 621.900	30		80 235.040	100	
70 640.660	40		80 291.320	30	slow -
70 676.500	30		80 302.880	50	
70 706.100	30		80 313.660	130	
70 728.700	30		80 385.080	100	
70 731.900	50		80 405.500	60	broad

80 414.780	40					
80 420.160	60			83 063	70	+
80 421.900	40			83 505.440	80	
80 433.120	40			83 701	40	
80 477.620	60 \			83 860.360	120	-
80 479.780	60 /			83 894.400	110	slow -
80 609	50 +			83 940.320	100	
80 843.060	70			83 995.680	60	
80 860.780	80					
81 212.740	60			84 168.475	80	-
81 241.560	160 \			84 205	60	
81 242.760	120 /			84 234.530	90	-
81 255.600	95			84 524.820	60	very slow +
81 283.760	150	-		84 788	60	-
81 368	30			84 919.120	210	very slow +
81 415	40			84 966	80	
81 488	30					
81 491	35			85 101	100	+
81 568	30			85 245.700	100	
81 571	30			85 265.660	100	
81 627.220	60			85 612	50	
81 629.600	60			85 637	50	
81 807	20			85 759	60	-
81 871.620	40			86 655	70	
81 876.870	45					
81 901	20			87 197.830	60	+
81 934.650	40			87 619.670	45	
81 941.900	20			87 677.590	40	
81 946.430	30			87 729	60	slow -
81 973	25			87 737	30	
82 008.440	60			87 757		
82 029.540	110			87 767		
82 058.760	60			87 821.900	60	slow +
82 075.900	50			87 886.850	70	broad
82 145.180	60					
82 165.780	50			88 003.200	40	
82 182.240	40			88 010.000	40	
82 283	40			88 066.710	130	
82 298	40			88 084.300	50	
82 348	120			88 101	60	
82 402.420	40	slow -		88 278	50	
82 418.160	70			88 337.600	70	
82 470.360	110	slow -		88 343.880	60	
82 481.100	40	slow +		88 349.800	50 \	
82 487.980	110			88 351.020	50 /	
82 623.800	30			88 444.740	30	slow -
82 670.160	60			88 462.020	100	
82 681.100	50			88 480.470	110	
82 789	40	slow -		88 520.210	170	
82 821.500	110			88 570.800	30	
82 890.340	50	slow +		88 586.200	30	
82 946.560	40	-		88 594.880	30	
82 964.380	100			88 743.700	30	

88 748.750	130		90 252.300	50 /
88 779.600	30	slow +	90 267.180	80
88 794.400	70		90 285.160	60 +
88 801.560	100		90 368.740	120
88 871.260	100		90 388.040	40
88 877.600	80		90 528.360	50
88 889.450	160		90 548.450	110
88 895.460	130		90 567.900	30 \
88 901.100	30		90 569.700	30 /
88 914.660	30		90 584.400	30 slow +
88 921.080	140		90 614.700	30
88 940.000	30		90 618.860	80
88 960.800	30		90 670.780	30
			90 680.700	50
89 010.920	130		90 710.670	60
89 034.360	100		90 728.300	30
89 079.260	70		90 741.920	65 slow ? +
89 106.900	30		90 747.900	40
89 114.000	30		90 784.700	30
89 118.800	40		90 813.020	45
89 143.420	40 \ ?		90 932	20
89 144.050	40 / ?			
89 191.160	220		91 001.220	50
89 211.800	30		91 015.100	30
89 258.600	30		91 020.920	110
89 279.620	240		91 027.360	110
89 329.670	220		91 035.520	50
89 359.880	180		91 075.440	80 \
89 377.860	130		91 077.860	80
89 388.660	110		91 079.560	50 /
89 426.180	130		91 100.620	100
89 438.780	160		91 105.360	40 slow +
89 443.760	30		91 115.180	50
89 455.400	190		91 122.740	50
89 474.700	30		91 143.220	140
89 505.900	30		91 153.820	80
89 515.620	170		91 172.760	160
89 551.560	40	+ -	91 186.860	60 \
89 634.840	130		91 191.200	70
89 665.620	70		91 197.000	80 /
89 670.660	160		91 208.160	160 \
89 685.100	80		91 211.140	80 /
89 717.980	160		91 216.740	50
			91 316.720	80
90 112.320	100 \		91 329.760	50
90 113.600	100		91 353.880	70 -
90 114.580	90 /		91 363.360	90
90 164.620	100		91 446.620	80
90 183.400	50 \		91 474.420	60
90 184.560	50 /		91 481.660	50
90 238.130	80		91 533.500	30 slow +
90 246.520	50 \		91 666.700	170
90 248.100	30		91 669.360	50
90 250.500	40		91 672.740	100

91 689.620	50		96 372	100	slow +
91 731.380	80		96 520	90	
91 760.320	70		96 635	100	
91 791.960	160		96 802	120	
91 831.200	160		96 807	60	
91 846.920	50		96 994	40	
92 029.000	30		97 042.240	180	
92 043.830	120	-	97 135.160	40	slow -
92 111.680	100		97 149.400	100	
92 120.100	100		97 158.780	110	
92 144.120	30	slow -	97 300.600	130	
92 155.960	30		97 319.840	60	
92 160.240	40	slow -	97 408.080	100	
92 175.440	70		97 427.540	100	
92 281.660	50		97 432.340	90	
92 719	90		97 539.400	110	
92 931	80		97 579.640	60	
92 943	60		97 640.800	100	
			97 677.620	30	
93 028	40		97 777.500	60	
93 305.040	130		97 883.920	60 \	
93 335.120	50	slow -	97 885.240	50 /	
93 401	40		97 896.340	60	
93 485.040	80		97 906.500	40 \	
93 796	30		97 907.980	40 /	
93 813.770	40	very slow +	97 920.380	50	
93 843.480	110	slow -	97 928.920	50	
93 909.580	30		97 929.720	290 \	
93 920.960	30		97 934.200	290 }	very slow +
93 926.860	30	slow-	97 941.800	210 /	
93 935.500	30		98 001.620	110	
93 952.800	60	slow +	98 013.960	70	
94 035	40		98 023.620	130	
94 144.800	40		98 031.160	30	
94 172.400	100	slow -	98 086.840	30	slow +
94 210.600	80	slow -	98 107.520	140 \	
94 354.580	60		98 120.960	140 }	very slow +
94 389.780	50		98 134.800	140 /	
94 435.460	140	slow -	98 246.500	30	
94 479.820	130	slow -	98 275.600	80	
94 706.040	110	+	98 278.920	30 \	slow -
94 837	50		98 281.120	20	slow -
94 909	40		98 283.400	7 /	slow -
			98 283.880	80	
95 169	40		98 293.120	130	
95 312	90	+	98 346.600	30	
95 362	90	slow -	98 368.280	190	CH3CHO ?98 367.696
95 606	90	broad	98 375.540	120	
95 854	50	slow +	98 377.360	120	
95 917	40	slow +	98 379.450	180	
			98 392.920	140	+
96 107	40	broad	98 399.800	90	

98 412.660	100		99 804.140	100	
98 437.920	130		99 825.220	40	
98 453.200	30		99 838.940	70	
98 454.840	90		99 877.780	140 \	
98 527.110	100	+	99 881.120	130 /	
98 623.800	30		99 902.640	130	
98 635.900	40	slow +	99 905.440	50	
98 651.140	180		99 924.820	50 \	
98 655.500	40		99 926.020	70 /	
98 671.500	30 \		99 955.100	100 +	
98 673.300	30		99 965.040	90 \ -	
98 676.100	30 /		99 968.480	60	
98 767.310	300	-	99 970.660	70 /	
98 781.820	60		99 995.440	90	
98 789.200	30		100 002.800	40	
98 791.040	30		100 004.640	60	
98 823.500	30		100 011.220	40	
98 832.400	30		100 014.360	100	
98 841.400	30		100 027.780	60 +	
98 851.700	250		100 053.320	60 \	
98 854.080	50		100 054.780	45	
98 867.360	30		100 055.900	45 /	
98 882.200	30		100 063.330	130	
98 888.900	30		100 070.660	80	
98 897.720	190		100 087.960	30	
99 001.180	25		100 129.780	50	CH3CHO 100 130.239
99 093	30		100 133.290	60	
99 198.330	150		100 144.040	40	
99 248	30		100 146.160	90	
99 347.960	120		100 156.890	60	
99 383.550	120		100 175.480	50	
99 391.540	65		100 184.330	210	
99 406.500	50		100 218.140	80 \	
99 422.840	65		100 220.780	80	
99 460.840	30		100 224.560	50 /	
99 472.600	30	+	100 234.620	100	
99 490.160	65		100 242.300	40 \	
99 524.840	160		100 245.120	60	
99 560.940	80		100 247.840	50 /	
99 573.640	50 \		100 324.860	90	
99 575.320	110 /		100 341.320	80	
99 583.510	200		100 351.200	130 \	
99 653.440	50		100 353.000	60 /	
99 660.160	50		100 363.400	80 \	
99 663.660	100		100 366.620	60 /	
99 711.480	40		100 384.380	80	
99 718.280	50		100 469.060	40	
99 728.800	90		100 474.620	100	
99 739.940	30	slow -	100 479.800	50 \	
99 750.380	50	very slow -	100 482.040	60 /	
99 765.360	90		100 506.180	90	
99 769.300	140 \		100 517.520	60	
99 771.120	170 /		100 524.280	85	

100 526.480	40		104 528.050	50	very slow +
100 610.560	140 \		104 557	70	
100 612.540	130 /		104 583	60	broad
100 616.820	100	slow -	104 590	40	slow +
100 638.760	60		104 814	90	slow +
100 646.440	100				
100 650.180	80		105 098	90	
100 674.260	180		105 246	90	
100 708.580	170		105 258	100	
100 759.380	90		105 354.100	40	-
100 775.920	60		105 385.900	320	
100 777.880	150		105 543.340	520	+
100 781.900	40		105 605.590	100	slow +
100 878.600	80		105 625.600	60	slow +
100 892.350	60		105 653.000	320	
100 901.050	40		105 665.030	40 \	
100 908.150	40		105 666.240	60 /	
100 922.750	40		105 754.830	600	- + 50 V
100 938.750	50	NH2CHO	100 922.291	105 773.680	200
100 952.300	130			105 775.700	50
100 960.880	250			105 800.600	50
				105 810.060	30 \
101 120.130	170			105 812.400	30 /
101 258.160	130			105 817.560	50
101 341	70			105 832.340	240
101 375.660	210			105 877.420	50
101 456.810	160			105 891.710	270
101 541	90			105 910.520	320
101 678	60			105 946.800	100
101 711.010	90			105 957.600	40
101 787.930	130			105 972.540	260
101 820	90				
			106 023.160	50	slow -
102 052	40		106 067.480	210 \	
102 064.230	80	NH2CHO	102 064.3	106 069.490	210 /
102 203	70	-		106 093.520	250
102 308.070	130			106 096.180	50
102 567.320	30	slow -		106 107.720	110
102 682.620	50	slow +		106 134.780	60
102 934.180	40	slow -		106 141.000	70
102 958	90			106 146.200	140
				106 151.860	100
103 008.910	100			106 172.240	210
103 223.400	50	slow +		106 183.860	40
103 448.280	100	slow -		106 300.200	290
103 642	60	slow -		106 307.180	130
103 808	50			106 358.600	40
103 821	50			106 396.820	70
				106 409.500	130
104 091	50			106 513.320	140
104 119	50			106 533.700	190
104 237	100	+		106 541.580	140
104 286	70			106 569.340	40
104 398	100			106 600.240	160

106 606.300	130	\	108 245.200	80	+
106 608.260	100	/	108 408.810	140	
106 715.330	160	\	108 418.360	50	
106 718.100	130	/	108 454.520	60	
106 751.820	220		108 492.890	130	
106 897.500	110		108 589.740	25	\
106 914.420	180		108 590.600	15	/
106 971.580	60		108 609.210	20	
107 013.820	45	CH3OH	107 013.85	108 704	50
107 017.780	75	+ -		108 740.720	90
107 023.790	50			108 748.540	30
107 034.590	270	+		108 797.380	100
107 036.840	25			108 804.300	45
107 041.740	40			108 809.760	25
107 044.620	40			108 822.510	40
107 045.600	30			108 857.940	40
107 057.110	160			108 919.760	160
107 107.770	230			108 937.100	30
107 123.320	190			108 943.300	100 \
107 175.460	30			108 944.690	100 /
107 178.960	30			108 959.820	100 \
107 182.330	180			108 960.360	100 /
107 195.370	130	+		109 009.880	30
107 232.560	100			109 019.890	60
107 243.680	170	\		109 031.040	130 \
107 245.010	160	/		109 031.740	130 /
107 364.620	40			109 040.910	130
107 367.280	110			109 048.640	130
107 372.860	30			109 072.210	100
107 376.020	30			109 105.870	40 \
107 377.090	110			109 108.050	40 /
107 419.570	20	slow -		109 115.140	50
107 448.280	60			109 121.480	40
107 494.240	140			109 126.610	20
107 499.420	80	\		109 127.680	50
107 500.560	60	/		109 138.720	35
107 559.510	100			109 149.850	40
107 582.110	90	-		109 162.900	30
107 619.800	160			109 187.050	50 \
107 746.040	50			109 188.250	50 /
107 797.340	130			109 194.900	40
107 814.940	50			109 198.720	20
107 845.700	150			109 209.450	50
107 870.520	160			109 238.080	60
107 904.630	250			109 263.400	100
107 949.920	100			109 269.950	50
107 956.490	230			109 274.500	40
107 973.200	60			109 278.240	40
107 989.320	40	slow +		109 283.400	40
108 010.540	25			109 361.800	50
108 014.780	15			109 367.750	40
108 028.930	65			109 372.250	30
108 238	90			109 375.870	50 \
				109 377.050	40

CH3OH 109 138.71

109 380.500	40	/		112 105.060	110	\	-
109 482.560	30	slow +		112 105.560	110	/	
109 538.620	50			112 114.860	180	-	
109 547.350	40			112 254.800	230	CH3CHO	112 254.48 6(1,6) - 5(1,5) E
109 553.360	60	slow +		112 287.110	100	HCOOH	112 287.12 5(2,4) - 4(2,3)
109 556.690	35			112 382.950	70		
109 604.660	60	slow -		112 432.400	100	HCOOH	112 432.30 5(4,2) - 4(4,1)
109 640.050	100			112 459.720	100	HCOOH	112 459.60 5(3,3) - 4(3,2)
109 692.980	45			112 466.920	100	HCOOH	112 467.00 5(3,2) - 4(3,1)
109 776.480	60	\		112 469.240	60		
109 779.540	80	/		112 543.670	70	slow -	
109 785.340	50			112 545.610	40		
109 806.940	50	\		112 567.750	30	slow +	
109 807.900	60	/		112 586.360	110	\	
109 824.660	40			112 587.460	70	/	
109 890.880	50			112 714.980	90	slow +	
109 905.580	70	slow +		112 727.560	70	broad	
109 956.140	30			112 775.500	35		
110 030.460	80			112 848.900	350	slow -	
110 089.140	160			112 860.800	30		
110 104.720	80			112 891.440	50	HCOOH	112 891.41 5(2,3) - 4(2,2)
110 110.920	100			112 896.080	80		
110 156.900	30			112 899.120	40		
110 164.240	40			112 926.390	70	slow -	
110 254.920	130			112 938.370	190	\slow -	
110 418.960	110			112 941.850	130	/slow -	
110 460.980	290			113 083	30	-	
110 523.580	30			113 108.920	160		
110 548.540	210			113 111.720	160	slow -	
110 619	60	-		113 157	60		
110 855	50			113 162	50		
110 948	50	slow +		113 232.000	70		
111 028.770	40			113 321.979	90		
111 047.550	40		broad	113 323.530	100		
111 133	60			113 379.100	90		
111 285	60			113 430.130	90	slow +	
111 319.480	40			113 492.410	90		
111 328.940	40			113 580	60	slow -	
111 336.240	40			113 660	90	slow +	
111 365.860	40			113 705	40	slow +	
111 367.860	130			113 736	90	slow +	
111 384.070	260	-		113 786	70		
111 402.420	60	slow -		113 841.170	45	slow +	HONO 113 841.03 5(1,5) - 4(1,4)
111 474.420	30	slow +		114 003.820	20	\slow +	
111 497.480	130			114 005.340	45	slow +	
111 514.590	170			114 006.940	7	/slow +	
111 540.660	40	slow +		114 019.200	30		
111 551.150	30	slow + ?		114 034.000	50		
111 723	20			114 043.160	200		
111 806.290	190	-		114 058.590	210		
111 899.300	240	-		114 069.080	30		
111 917.140	30	slow -		114 123.790	260		
111 923.860	40	slow +		114 134.940	50		
111 982.190	50	very slow -		114 141.220	30		

114 148.700	80 \	115 426.300	60
114 149.640	40 /	115 434.570	200
114 166.400	40	115 462.540	50
114 233.020	50	115 563.040	30
114 278.150	350	115 628.420	140
114 312	50 broad	115 634.620	80 slow +
114 408.960	100 broad	115 710.560	15 \slow +
114 471.280	160 slow -	115 711.640	15 slow +
114 534.600	40 broad	115 712.720	15 /slow +
114 576.380	260	115 716.520	170
114 582.860	70 broad	115 725.860	140 C2H5CN-? 115 725.965
114 589.500	30	115 734.210	160
114 598.240	230	115 804.740	90 slow +
114 602.520	70	115 810.300	30
114 643.920	30	115 815.880	140
114 650.880	30	115 843.800	40
114 662.700	100	115 846.760	110
114 727.400	260	115 856.400	100
114 736.370	150	115 881.500	140
114 748.000	200 \	115 892.060	60
114 749.160	200 /	115 902.440	50
114 750.560	40 CH3OH 114 750.70	115 924.960	80
114 764.940	40	115 934.860	65
114 786.980	170	115 938.380	50
114 803.120	110	115 960.220	290 \
114 806.620	30	115 962.900	140 /
114 816.020	80 \	115 971.180	90
114 818.700	50	116 119.600	130
114 832.840	30	116 161.390	270
114 843.350	180	116 173.010	100
114 890.300	30	116 176.870	280 \
114 893.780	40 slow +	116 178.020	250 /
114 903.770	60 slow -	116 235.590	280
114 906.900	50	116 238.160	260
114 975.580	30	116 241.340	260
114 996.290	190	116 309.500	40
115 019.130	160	116 340.050	90
115 036.920	70	116 345.750	30
115 061.660	90	116 378.050	30
115 063.170	20	116 388.100	30
115 070.780	200	116 412.080	180
115 106.330	65	116 447.470	120
115 110.810	200	116 514.050	170
115 119.750	200	116 565.170	160
115 144.120	65	116 618.320	100 \
115 146.740	200 slow -	116 619.610	90 /
115 155.180	200	116 646.720	20 \
115 203.850	260	116 647.570	100 /
115 291.540	20 \slow +	116 711.440	15 CH3CHO 116 711.450
115 293.540	25 slow +	116 715.270	150
115 295.520	15 /slow +	116 725.650	160
115 338.220	160 \	116 757	60 +
115 339.960	320 /	116 786.080	120
115 410.120	100	116 922.500	50

116 953.750	25		124 948	80	
117 137.360	50				
117 143.060	80		125 035.520	80	
117 149.600	60		125 062.940	120	
117 225.700	50		125 215	80	
117 281.700	70	slow -	125 318	100	
117 383.050	210		125 538	80	2 lines
117 436.770	90		125 684	100	
117 467.710	180		125 819	70	
117 514.420	180		125 887	80	
117 602.290	25				
117 605.600	30		127 553	80	
117 615.300	30				
117 626.600	30		131 155	50	
117 630.200	40		131 353	60	
117 641.000	30		131 508	90	+
117 651.940	50		131 618	40	slow +
117 678.420	100		131 628	70	
117 738.700	50		131 751	60	
117 741.200	60		131 813	90	
117 760.200	60	+ -	131 920	70	
117 766.360	50				
117 769.880	30		133 545	90	
117 777.000	30		133 556	100	broad
117 816.520	80		133 644	100	broad
117 831.890	170		133 712	60	-
117 842.380	80		133 722	80	
117 847.220	80	slow +			
117 870.980	80		134 105.020	80	
117 903.000	80		134 131.260	110	
117 911.760	40		134 139.980	190 \	
118 003.280	70		134 142.300	200 /	
118 006.420	70		134 165.700	80	slow -
118 026.610	50		134 201.880	200 \	
118 039.100	70		134 204.300	250 /	
118 070.770	40		134 256.220	100	
118 078.310	50		134 280.220	150	
118 086.470	50		134 348	100	
118 092.200	7	CH3CHO	118 092.403		
118 093.840	40		134 409.800	80 \	
118 098.440	50 \		134 414.600	80 /	broad
118 099.640	50	/HCOOCH3	118099.557		
123 508	40		134 436.000	200	slow +
123 648	40		134 468.800	100	
123 789	90	broad	134 481.520	450	very slow HNCO
			134 565	80	
			134 606.400	70	slow -
			134 642.320	90	
124 085	80		134 676.080	90	
124 253	80		134 713.120	70	broad
124 306	80		134 720.420	80	
124 424	80		134 784.100	140	
124 455	80		134 788.880	160	
124 511	90		134 815.900	50	
124 905	90		134 830.000	130	
124 927	80		134 842.340	260	

134 870.980	200		143 519	60 /
134 968.640	220 \	-	143 577	100
134 971.620	100 /		143 582	100
134 980.440	200		143 589	90
135 101	150		144 133	90
135 356	200		144 272	70
135 394	150		144 439	60
135 443	100		144 483	60
135 597	150		144 681	70
135 612.100	80	broad	144 827.920	150 \ slow ?
135 618.300	80		144 833.900	80 / slow ?
135 648.440	100		144 906	100
135 682.440	130		145 116	100
135 705	60		145 225	150
135 738	60		145 370.000	70
135 772	90		145 389.700	250 H2CO nu5
135 895	60		145 450.600	80
136 210	90		145 459.740	80
136 234	80		145 477.300	130
136 466	60		145 481.240	130 very slow +
136 497	60		145 505.420	60
136 550	50	+	145 519.660	60
136 594	60		145 535.220	90
136 644	80		145 551.180	80
			145 563.900	180
140 721.180	60		145 574.180	200
140 735.000	70		145 618.930	150
140 752.800	150		145 650.260	500 slow +
140 763.310	1300		145 664.400	150
140 808	130		145 681.300	80
			145 685.820	80
142 015	70		145 703.780	60
142 030	70		145 710	90
142 112	60		145 715	90
142 129	60		145 732.500	80
142 228	80		145 749.140	80
142 414	80		145 762.300	90
142 502	70		145 766.180	100
142 511	130		145 769.900	90
142 736	60		145 789.900	100
142 740	60		145 792.520	150
142 746	60		145 811.400	70
142 838	70		145 819.520	80
142 845	80		145 826.600	100
142 860	80		145 836.400	100
142 883	90		145 839.840	400 very slow +
142 896	70		145 910.500	40 +
			145 937.000	60
143 108	60		145 943.400	100 \
143 436	80		145 946.220	100
143 454	80		145 947.540	100 /
143 517	60 \		145 962.940	100

145 971.220	30	-	149 820	100	-
145 973.900	30		149 928	150	-
145 983.200	60				
145 988.540	60		150 021	150	
			150 094	190	
146 145.200	100	slow +	150 129.820	130	-
146 167.400	50		150 141.600	40	
146 175.640	60		150 150.000	300	
146 186.000	50		150 156.960	400	
146 507	70		150 206.800	70	
146 581	60		150 235.200	70	
146 686	60		150 268.720	70	
146 679	70		150 280.020	100	
146 673	50		150 297.080	240	
146 734	90		150 320.700	50	
146 837	80		150 330.000	60	
146 855	80		150 341.120	300	
146 862	80		150 383.840	100	
146 981	70	slow +	150 418.125	600	
			150 522.380	180	
147 209	60		150 562.240	100	
147 239	60		150 575.040	200	
147 329	130		150 600.620	150 \	
147 476	100		150 602.180	150 /	
147 566	90		150 626.340	200	
147 590	70		150 787.400	60	slow -
147 596	70		150 793.860	150	
147 618	100		150 794.820	110	very slow +
147 691	80		150 998	150	
147 761	200				
147 879.740	200	-	175 884.325	120	slow
148 069	90				
148 157	80				
148 347	80				
148 350	80				
148 544	70				
148 578	80				
148 598	70				
148 667	60				
148 696	70				
148 783	60				
148 993	150				
149 031	70				
149 086	70				
149 137	70	+			
149 163	60	+			
149 225	100				
149 234	100				
149 342	60				
149 381	100				
149 409	100				
149 607	70				